Two Interferons Alpha Influence Each Other during Their Interaction with the Extracellular Domain of Human Type Interferon Receptor Subunit 2[†]

Hana Schmeisser,*,‡ Inna Gorshkova,§ Patrick H. Brown,§ Peter Kontsek,‖ Peter Schuck,§ and Kathryn C. Zoon‡

National Institute of Allergy and Infectious Diseases and National Institute of Biomedical Imaging and Bioengineering, National Institutes of Health, Bethesda, Maryland 20892, and Institute of Neuroimmunology, SAS, Bratislava, Slovak Republic

ABSTRACT: The interaction between two human interferons alpha (IFN-αs) and the extracellular (EC) domain of human type I IFN receptor subunit 2 (IFNAR2) was analyzed. Previous experiments using Daudi cells showed that IFN-α21b and some IFN-α hybrids (made from IFN-α2c and 21b) competed poorly for the IFN-α2b binding site. This study examined the causes of the poor competition between these IFN-αs. IFN-α2c and the IFN hybrid CM3 {IFN-α21b(1−75)(81−95)/IFN-α2c(76−80) (96−166), Y86K} were selected for this study based on their cell binding and biological properties. Competitive binding ELISA, native electrophoresis followed by Western blot, electrospray ionization mass spectrometry (ESI-MS), surface plasmon resonance biosensor (SPR) analysis, as well as neutralization of antiproliferative activities on Daudi cells in the presence of soluble IFNAR2-EC show evidence that each of the described IFN-α subtypes affected the binding of the other IFN-α to IFNAR2-EC by affecting the stability of the complex, i.e., dissociation of the complex. Moreover, native electrophoresis with different IFNAR2-EC mutants showed that IFN-α2c and CM3 utilize different amino acids in the binding domain of IFNAR2-EC. In addition to that, analytical ultracentrifugation (AUC) revealed differences in the oligomeric state of the two studied interferons. Our results demonstrated that two individual IFN-αs interact differentially with IFNAR2-EC and influence each other during this interaction. This study contributes to the understanding of the mutual interaction between multiple IFN-α subtypes during the competition for binding to the receptor.

In mammals, the type I IFNs are grouped into five major classes: α, β, ε, κ, ω (1−3). They are induced in all nucleated cells in response to viral and bacterial infections, natural and synthetic double-stranded RNA, mitogens, protozoa and certain cytokines (3, 4).

Human IFN-α is represented by a group of related subtypes, encoded by a multigene family comprising 14 nonallelic genes. At the protein level, there is 75%−99% identity in the primary structure of human IFN-α species (5−7). Individual subtypes show quantitatively distinct spectra of antiviral, antiproliferative and immunomodulatory activities (8−11). The existence of the numerous subtypes of IFN-α may provide a fine mechanism of regulating the biological effect of IFN.

The type I IFNs bind with distinct affinities to the common type I IFN receptor complex (IFNAR), expressed on the surface of target cells in low numbers (100−5000 molecules/cell) (12−14). Functional human IFNAR is a heterodimeric complex composed of two transmembrane polypeptide chains, IFNAR1 and IRNAR2, with distinct complementary functions, which associate to form a heterodimer upon IFN-binding (7, 15). The IFNAR1, with a molecular weight of 110−130 kDa, has a very low affinity for IFN-αs ($K_D \sim 10^{-6}$ M). IFNAR1 alone binds only one species of IFN-α (α8), but is required for signaling by all type I IFNs (16). The second component, IFNAR2, has a molecular weight of 95 kDa. The protein alone displays a relatively high affinity for binding of IFNs ($K_D \sim 10^{-9}$ M) and is the major ligand-binding receptor subunit (13). The dimerization of IFNAR2 with IFNAR1 results in a fully functional receptor, and its binding affinity increases by approximately 100-fold ($K_D \sim 10^{-11}$ M).

Previously, the antiproliferative and competitive binding activities of 20 purified components of human lymphoblastoid IFN were compared with that of recombinant human IFN-α2b on Daudi and AU937 cells (12). Moreover, differences between IFN hybrid molecules (derived from IFN-α2c and IFN-α21b) in competition for receptor binding site were reported (17).

Most recent studies were focused on detailed mapping of interferon receptor binding site (18−24). However, little is known about the mutual interaction among different IFN-α subtypes during the process of binding to the receptor.

The aim of this study was to understand the interaction between two distinct IFN-αs and IFNAR2-EC. To this end, we applied several different assays (ELISA, SPR, native electrophoresis followed by Western blot, ESI-MS, AUC), each of which highlighting select aspects of the interactions.

* To whom correspondence should be addressed. NIH/NIAID, HFM 8001, 50 Center Drive, Building 50, Room 5515, Bethesda, MD 20892. Tel: 301-402-5369. Fax: 301-594-6496. E-mail: hschmeisser@niaid.nih.gov.
‡ NIAID, NIH.
§ NIBIB, NIH.
‖ Institute of Neuroimmunology, SAS (deceased, September 2005).

Taken together, a complex picture of the interaction emerged with features previously unrecognized. Although the detailed mode of interaction in the membrane is still unclear, our study revealed evidence for differences in IFN/IFN/receptor complex stability, e.g., the mutual influence between IFN-α subtypes during their binding to IFNAR2-EC. Moreover, IFNAR2-EC mutants showed that the studied IFN-αs bind to the IFNAR2-EC with distinct binding centers.

EXPERIMENTAL PROCEDURES

Cell Lines. Human Daudi cells were a gift from Dr. P. Grimley (Department of Pathology, Uniformed Services University of the Health Sciences, Bethesda, MD). Bovine kidney MDBK cells were obtained from the American Type Cell Culture Collection (ATCC, Manassas, VA). Daudi and MDBK cells were cultured in RPMI 1640 medium (GIBCO, Invitrogen Corp., Grand Island, NY) with 10% fetal bovine serum (GIBCO), 2 mM glutamine (GIBCO) and 0.2% gentamicin (Cambrex Bio Science, Walkersville, Inc., MD). Cells were incubated at 37 °C in a humidified atmosphere containing 5% CO_2. All cells were determined to be free of mycoplasma.

Interferons. Recombinant IFN-α2c, IFN-α2c-6-histidine-tag, and hybrids IFN-α21b (1−75) (82−95)/IFN-α2c (76−81) (96−166) with Y86K (designated CM3), and CM3-6-histidine-tag were generated as previously described (*17*, *24*). Specific activities of IFNs on MDBK were 4.9×10^8 (IFN-α2c), 3.2×10^8 (IFN-α2c-6-histidine-tag), 2.8×10^8 (CM3), and 3.5×10^8 (CM3-6-histidine-tag) IU/mg protein. Preparation and purification of IFNs was described previously (*17*, *24*). Ellman assays (*25*) under native and denaturing conditions were performed to assess free cysteine residues. The purity of the IFNs was evaluated by SDS−PAGE under reducing and nonreducing conditions followed by staining with Coomassie R-250 (Pierce, Rockford, IL). Samples were incubated for 5 min at 90 °C with or without NuPAGE sample reducing agent (Invitrogen, Carlsbad, CA) and resolved on 10−20% tris-glycine gel (Invitrogen). Novex Tris-Glycine SDS Running Buffer (Invitrogen) and Novex Tris-Glycine SDS Sample buffer (Invitrogen) were used for SDS−PAGE. Protein in IFN samples were evaluated using the Bradford protein quantification assay (Pierce). The order of the N-terminal amino acids was confirmed by protein sequencing.

Soluble IFNAR2-EC. The EC domain of human type I IFN receptor subunit 2 (IFNAR2-EC) and IFNAR2-EC mutants (I47A, M48V and I105A) were a generous gift from Dr. G. Schreiber. Expression and purification have been described by Piehler (*21*).

Monoclonal Antibodies. The following murine monoclonal antibodies were used: mAb N27 (epitope 43−53) against IFN-α2c (*26*), mAb NK2 (epitope 112−132) against human leukocyte IFN (*27*), mAb 1−36 (epitope 63−85) against human IFN-α1 (*28*), mAb 4F2 (epitope 113−149) against consensus IFN-α (*9*) and mAb III/21 against a synthetic fragment 151−165 of IFN-α1 (*29*). All antibodies have IFN-neutralizing activity except mAb III/21, and were used as hybridoma culture supernatants containing respective antibodies at concentrations of 5−10 μg/mL. MAb 46.10 against soluble IFNAR2-EC (*13*) was kindly provided by Dr. D. Novick. Monoclonal antibody NK2 was obtained from Lonza

Biologics PLC Slough, Berkshire, U.K., mAb III-21 was a generous gift of Dr. H. Arnheiter (National Institute of Neurological Disorders and Stroke, NINDS) and mAb 4F2 was kindly provided by Dr. E. Swanson (Amgen, Thousand Oaks, CA).

Solid Phase IFN ELISA and Sandwich IFNAR2-EC ELISA I. In solid phase IFN ELISA (used as control), Immulon 2HB microtitration plates (Dynatech Laboratories Inc., Chantilly, VA) were directly coated overnight at 4 °C with IFNs (3 μg/mL, 50 μL/well in PBS), and then specific mAbs (C- or N-terminal) were added. In the sandwich IFNAR2-EC ELISA I, Immulon 2HB polystyrene microtitration plates were coated overnight at 4 °C with IFNAR2-EC (3 μg/mL, 50 μL/well in phosphate-buffer saline−PBS, pH 7.2); then IFNs (10 μg/mL, 50 μL/well in PBS) were added, followed by specific anti-IFN (C- or N-terminal) mAbs. The next step was repeated in all our ELISA experiments: After incubation for 1 h at 37 °C, the plates were washed, and secondary peroxidase-labeled goat anti-mouse IgG (H+L) antibodies (diluted 1:1000) were added, followed by incubation for 1 h at 37 °C. Positive reactions were visualized by the addition of 2,2′-azino-di-3-ethylbenzthiazoline-6-sulfonate (ABTS) peroxidase substrate solution {Protein Detector ELISA Kit (HRP, ABTS System) (Kirkegaard and Perry Laboratories, Gaithersburg, MD)}. Absorbance at 405 nm was measured in an ELISA microplate reader. Measurements were performed at least three times, and the results were consistent with data from representative experiments shown in the figures.

Sandwich IFNAR2-EC ELISA II. The sandwich IFNAR2-EC ELISA II was used to titrate the binding of the designated IFNs to the IFNAR2-EC. Immulon 2HB polystyrene microtitration plates were coated overnight at 4 °C with a concentration of IFNAR2-EC (3 μg/mL, 50 μL/well in PBS). Interferons IFN-α2c-6-histidine-tag (1−18 μg/mL) or CM3-6-histidine-tag (10−180 μg/mL) were then added at a volume of 50 μL/well in PBS, followed by the specific anti-IFN mAbs. After incubation at different time intervals (1, 2, 3 and 4 h) at 37 °C, the plates were washed, and secondary antibodies were added, followed by incubation for 1 h at 37 °C. Positive reactions were visualized and absorbance was measured as described above.

Competitive Sandwich IFNAR2-EC ELISA. Immulon 2HB Polystyrene microtitration plates were coated overnight at 4 °C with a concentration of IFNAR2-EC (3 μg/mL, 50 μL/well in PBS). Then, IFN-α2c-6-histidine-tag or CM3-6-histidine-tag was added at a concentration of 15 or 150 μg/mL, respectively (50 μL/well in PBS). After incubation for 3 h at 37 °C, the plates were washed and the second IFN (IFN-α2c-6-histidine-tag, 1−15 μg/mL or CM3-6-histidine-tag, 10−150 μg/mL) in PBS 50 μL/well was added. After incubation for 1 h at 37 °C, the plates were washed. A specific mAb targeted against the second IFN was added, and incubated for 1 h at 37 °C. Plates were washed, and secondary antibodies were added, followed by incubation for 1 h at 37 °C. Positive reactions were visualized and absorbance was measured as described above.

Competitive Binding Study by Biosensor Analysis. SPR experiments were performed with a BIAcore 3000 optical biosensor at 25 °C in the running buffer HBS (10 mM HEPES, pH 7.4, 150 mM NaCl, 1 mM EDTA, 0.005% P20). CM5 Sensor chips with a carboxymethylated dextran matrix,

EDC, NHS and P20 surfactant were obtained from BIA-CORE AB (Piscataway NJ). Proteins (IFNAR2-EC, IFN2-α2c or CM3) were covalently attached to the chip surface by amino coupling. At a flow rate of 10 μL/min, 70 μL of the mixture of freshly thawed EDC and NHS was employed to activate the surface, followed by the injection of the corresponding protein that was diluted into 10 mM NaOAc buffer pH 4.5 at a concentration of 30−35 μg/mL. The protein injection was stopped when the desired immobilization level was reached (∼1250, 2700 and 5900 RU for IFNAR2-EC, IFN-α2c and CM3, respectively). Then, each surface was deactivated by 70 μL of 1 M ethylenediamine pH 8.5 and washed thoroughly with HBS. The reference surfaces, which were treated with NHS/EDC and ethylenediamine, were generated on each sensor chip. Approximately 50% of the preconcentrated IFN-α2c (or CM3) became irreversibly attached to the chip surface; typically ∼25% of the immobilized IFN-α2c (∼30% of CM3) was active and could reproducibly bind IFNAR2-EC in HBS within at least a day. Approximately 70% of the preconcentrated IFNAR2-EC became irreversibly attached to the chip surface; typically ∼35%−50% of the bound IFNAR2-EC was active in binding of IFN-α2c or CM3. The behavior of the immobilized proteins was in overall agreement with previously published data for IFN-α2c and IFNAR2-EC interaction, which was studied by RIfS optical biosensing (21, 22).

To detect the interaction in HBS buffer, a sample volume of 20 μL of IFNAR2-EC, IFN-α2c, and CM3, separate or mixed, was injected at a flow rate of 5 μL/min onto the surface with the counterpart immobilized. Then, the surface-bound complex was allowed to dissociate. In some experiments, soluble IFN-α2c or CM3 was added in the dissociation phase allowing it to interact with the surface-bound receptor and the receptor−interferon complex (see details in the legends to figures). In the latter experiments, in order to control for the absence of oligomers or aggregates in the interferon samples, experiments were conducted with and without an additional FPLC purification step prior to the SPR studies, without significant differences in the observed binding traces. The response from the reference surface was subtracted from that of each of the experimental surfaces to correct for refractive index changes, matrix effects, nonspecific binding, injection noise, and baseline drift.

For a quantitative characterization and comparison of binding curves, initially the model of a simple bimolecular reaction was fitted to the data to estimate apparent kinetic and equilibrium constants (30). However, as outlined in the Results section, a more complex binding mode is present, and as a consequence we do not believe these apparent binding constants reflect the molecular properties.

Self-Association State of IFNs in Solution by Analytical Ultracentrifugation. Solutions of IFNs were prepared by serial dilution of a concentrated stock that had been passed through a size exclusion column (TSK-GEL) to 0.8, 0.4, and 0.1 mg/mL for IFN-α2c and 1.0, 0.5, and 0.1 mg/mL for CM3 using 10 mM HEPES (pH 7.1), 150 mM NaCl) as column running buffer. Three hundred ninety microliters of these solutions were loaded into double-sector charcoal-filled Epon centerpieces with SEC column running buffer as the reference solution. Samples were spun in an Optima XLI (Beckman Coulter) analytical ultracentrifuge at 20 °C and 50,000 rpm while the time- and radial-dependence of the

resulting concentration gradient was acquired using absorbance detection. Data analysis was performed utilizing the software Sedfit (vs.10.01; www.analyticalultracentrifugation.com) to obtain sedimentation coefficient distributions $c(s)$ with root-mean-squared deviations (rmsd) of all fits below 0.007. Integrated weight-average sedimentation coefficients were uncorrected for buffer density or viscosity or for the partial specific volume of the specific interferon, the default settings of 1.00 g/mL, 1.002 cP, and 0.73 mL/g, respectively were utilized. Global fitting of the sedimentation velocity data for IFN-α2c at all three concentrations was performed using the global analysis software SEDPHAT (31). The raw data were modeled with Lamm equation solutions that described sedimentation of a monomer−dimer−tetramer interaction scheme with rapid disassociation kinetics (31). The molecular weight of the monomer was fixed at 18.4 kDa (the value obtained for a CM3 monomer), while the sedimentation coefficients and binding constants of the IFN-α2c oligomeric species were allowed to float during the optimization process. The quality of the fit was judged by the magnitude of the root-mean-square deviations of the fit to the raw data (rmsd ≤0.0054), and by the randomness of the residuals.

Native Electrophoresis and Immunoblot. IFNAR2-EC (0.04 nmol), IFN (0.05 nmol) or IFN receptor complex were loaded onto 10% tris-glycine gel without SDS (Invitrogen) and run under native electrophoresis conditions (125 V, approximate current 6−12 mA/gel for 2 h). Novex Tris-Glycine Native Running Buffer (Invitrogen) and Novex Native Tris-Glycine Sample buffer (Invitrogen) with complete absence of denaturants were used. For preparation of IFN receptor complex either 0.05 nmol of IFN was incubated with 0.04 nmol of IFNAR2-EC at 37 °C for 1 h or 0.05 nmol of the first IFN was incubated with 0.04 nmol of IFNAR2-EC and then 0.05 nmol of the second IFN was added for an additional hour at 37 °C. For the different sample mixtures, final concentrations in the reaction volume were between 6.5 and 9.5 μM for IFNAR2-EC and 8.1−13.5 μM for each IFN. In experiments with IFNAR2-EC mutants, final concentrations in the reaction volume were between 7.3 and 10.0 μM for IFNAR2-EC mutants and 9.1−12.5 μM for each IFN. After native gel electrophoresis, gels were either stained using Sypro Ruby (Molecular Probes, Invitrogen Corp., Eugene, OR) and destained (10% methanol/7% acetic acid for 30 min), or processed for immunoblotting. Polyvinyldifluoride (PVDF) membranes (Bio-Rad Laboratories, Hercules, CA), Novex Tris Glycine Transfer Buffer (Invitrogen) supplemented with 20% methanol were used for immunoblot. Proteins were blotted with a constant voltage of 25 V for 2 h. After blocking with nonfat dry milk (Bio-Rad), the membranes were incubated for 1 h with supernatants containing different N-terminal anti-IFN mAbs, at concentrations of 5−10 μg/mL. Peroxidase-labeled goat anti-mouse IgG (H+L) (Southern Biotech, Birmingham, AL) diluted 1:4000 was used as secondary antibody. Signal was detected with SuperSignal West Pico kit (Pierce). For detection of histidine-tagged recombinant IFNs, nickel-activated horseradish peroxidase (HisProbe-HRP) and SuperSignal West His probe TM Kit (Pierce) were used.

Stained membranes were visualized with a LAS-3000 CCD camera system (FUJIFILM Medical Systems, Stamford, CT), and gels were visualized on a UV lamp at 260−290

nm and digitized using a Kodak EDAS 290 (Eastman Kodak, Rochester, NY). After detection of signal, PVDF membranes were restored in Western blot stripping buffer (Pierce) and reprobed.

Electroelution. IFN−receptor complexes (0.5 nmol of each IFN + 0.4 nmol of IFNAR2-EC) were run in a native gel (10% Tris-Glycine, 5-well gels) under conditions described above. Gels were stained with Sypro Ruby (Invitrogen) and gel slices containing the protein complexes were excised and transferred into GeBAflex- midi tubes with 3500 Da cutoff (Gene Bio-Application Ltd., Kfar-Hanagid, Israel). Electro-elution was done in Novex Tris-Glycine SDS Running Buffer (Invitrogen) in horizontal electrophoretic apparatus 2 h/100 V and reverse polarity for 120 s, using Gel extraction kit (Gene Bio-Application Ltd.). After electroelution, protein solution was transferred into a fresh tube for trichloroacetic acid (TCA) precipitation to prepare samples for mass spectrometry (MS) as described in Gel extraction handbook (Gene Bio-Application Ltd.). To increase protein precipita-tion yield, samples were incubated overnight at −20 °C with 98% acetone. After air-drying, the pellet was resuspended using 20 μL of 0.1 M NaOH. Samples were analyzed by reducing SDS−PAGE using 10−20% Tris-Glycine gels (Invitrogen), as described earlier, followed by Sypro Ruby staining (Invitrogen), or mass spectrometry.

Protein Identification by Mass Spectrometry. Protein identification of 1D gel separated proteins was performed on reduced and alkylated, trypsin digested samples prepared by standard MS protocols. Tryptic digests were analyzed by coupling the Nanomate (Advion BioSciences, Ithaca, NY), an automated chip-based nanoelectrospray unit, to a quad-rupole-time-of-flight mass spectrometer QStarXL MS/MS System (Applied Biosystems/Sciex, Framingham, MA). Computer-controlled data-dependent automated switching to MS/MS provided peptide sequence information. AnalystQS software (Applied Biosystems/Sciex) was used for data acquisition. Data processing and databank searching were performed with Mascot software (Matrix Science, Beach-wood, OH). The NCBInr protein database from the National Center for Biotechnology Information, NLM/NIH was used for the search analysis.

Antiviral and Antiproliferative Assays, and Neutralization of Antiproliferative Activities of IFNs with Soluble IFNAR2-EC. Antiviral and antiproliferative assays were performed as previously described (*9, 12, 32*). MDBK cells were used for antiviral assays. All IFN units are expressed with reference to the NIH human recombinant IFN-α2a standard Gxa01−901-535. For the antiproliferative assay, Daudi cells were treated with a single IFN at the initial concentration 360 ng/mL. For neutralization of antiproliferative activity, Daudi cells were mock treated or treated with IFN-α2c, CM3, or their mixture (tenfold dilutions from an initial concentra-tion of 360 ng/mL for single IFN, or 360 ng/mL + 360 ng/mL from equimolar IFNs mixture) with or without IFNAR2-EC (at a constant concentration of 5 μg/mL). Concentrations of IFNs that inhibit cell growth by 50% were calculated at 48 h time point.

RESULTS

Examination of the interaction between two IFN-αs and IFNAR2-EC by ELISA. To test whether two IFN-αs could differentially interact with IFNAR2-EC, a competitive

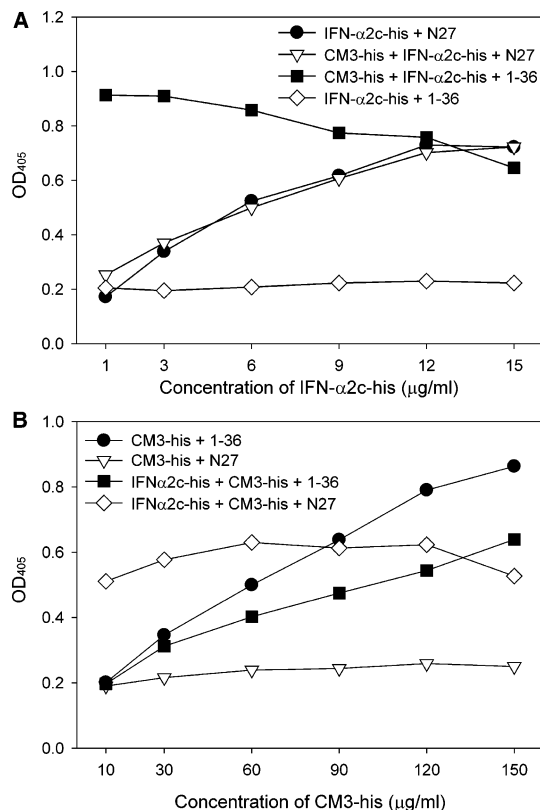FIGURE 1: A. Reactivity of IFN-α2c with IFNAR2-EC preincubated with CM3 (150 μg/mL) in competitive sandwich ELISA. Each data point represents the mean of three replicate assays (triplicates) from a representative experiment. B. Reactivity of CM3 with IFNAR2-EC preincubated with IFN-α2c (15 μg/mL) in competitive sandwich ELISA. Each data point represents the mean of three replicate assays (triplicates) from a representative experiment.

sandwich IFNAR2-EC ELISA was developed. The following criteria needed to be fulfilled: (1) Each of the IFNs should be specifically recognized by a specific anti-IFN monoclonal antibody after interaction with IFNAR2-EC. (2) An antibody selected for one IFN-α subtype should not exhibit any significant cross-reactivity with the other subtype. Based on these criteria and results from sandwich IFNAR2-EC ELISA I (Supplement 1, Supporting Information) the following IFN pair was selected: IFN-α2c-6-histidine-tag, specifically recognized by mAb N27 (epitope 43−53), and hybrid CM3-6-histidine-tag, specifically recognized by mAb 1−36 (epitope 63−85). Neither mAb N27 nor mAb 1−36 cross-reacted with the other IFN. This IFN pair was used to address the question whether there is a kinetic influence between IFN-αs during interaction on IFNAR2-EC.

Conditions for saturation of immobilized IFNAR2-EC with the IFN pair (IFN-α2c-6-histdine-tag, CM3-6-histidine-tag) as well as monoclonal antibodies (N27, 1−36) were deter-mined using a sandwich IFNAR2-EC ELISA II. Incubation of 15 μg/mL of IFN-α2c-6-histidine-tag or 150 μg/mL CM3-6-histidine-tag for 3 h completely saturated 3 μg/mL of coated IFNAR2-EC (Supplement 2, Supporting Information). The 3-hour incubation required to saturate IFNAR2-EC is in agreement with recently published data (*33*). Based on these findings we developed a competitive sandwich IF-NAR2-EC ELISA to examine the binding of two IFN species (CM3-6-histidine-tag and IFN-α2c-6-histidine-tag) to the receptor subunit IFNAR2-EC.
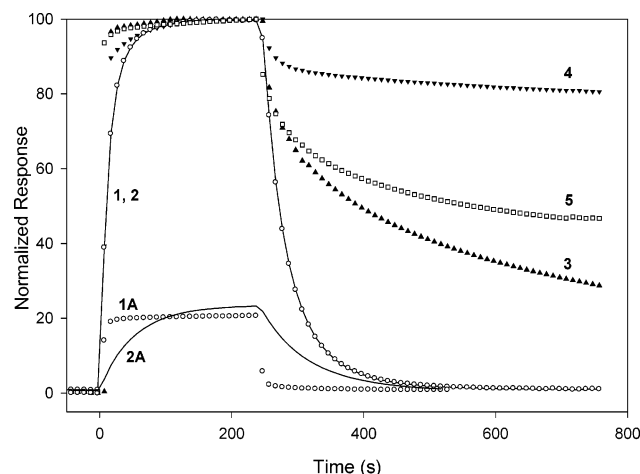
FIGURE 2: Comparative binding of IFNAR2-EC to IFN-α2c or CM3 immobilized on the chip surface and vice versa, measured by SPR. 700 nM IFNAR2-EC in the absence or the presence of soluble IFN-α2c or CM3, respectively, were injected onto the chip surfaces to which 2700 RU IFN-α2c (1, 1A, open circles) or 5900 RU CM3 (2, 2A, solid line) were immobilized; 800 nM IFN-α2c (3) or 800 nM CM3 (4) or their mixture (5) were injected onto the chip surfaces to which 1200, 1345 RU and 1230 RU of IFNAR2-EC, respectively, were immobilized. Data were normalized to set the maximal response to 100 for comparative purpose, every 10th point is shown. The R_{max} value (in RUs) was ~600 (1), 1800 (2), 690 (3), 560 (4), and 530 (5), respectively.

In those experiments, the receptor subunit was immobilized on the ELISA plate. The results from the competitive sandwich IFNAR2-EC ELISA were compared with those from the sandwich IFNAR2-EC ELISA (where IFN-α2c-6-histidine-tag or CM3-6-histidine-tag had been added to IFNAR2-EC at different concentrations). We found that after saturation of IFNAR2-EC with CM3-6-histidine-tag, the receptor subunit was still able to bind IFN-α2c-6-histidine-tag with low displacement of CM3-6-histidine-tag (Figure 1A, curve: CM3-his + IFN-α2c-his + 1−36). However, after IFNAR2-EC was saturated with IFN-α2c-6-histidine-tag, the binding of CM3-6-histidine tag was less effective (Figure 1B, curve: CM3-his + IFN-α2c-his + 1−36). The data appear to show that two IFN-α subtypes could bind simultaneously to IFNAR2-EC without significantly affecting each other's binding to IFNAR2-EC. Since ELISA is a semiquantitative method, a more precise method (SPR) was employed to clarify this observation.

Analysis of IFN-α2c and CM3 Interaction with IFNAR2-EC by SPR. To study the interaction of IFN-α2c and CM3 with IFNAR2-EC in real-time and with direct detection of surface-bound protein, we used a surface plasmon resonance biosensor. First, we immobilized IFN-α2c or CM3, respectively, on the sensor chip surfaces and then examined their interaction with IFNAR2-EC, which was in solution. Traces #1 and #2 in Figure 2 show the binding of IFNAR2-EC at a concentration of 700 nM, which was found to be virtually saturating receptor binding in the above ELISA assay. The binding of IFNAR2-EC to each of the immobilized interferons was significantly inhibited by the addition of soluble IFN-α2c (1600 nM) or CM3 (900 nM) to the receptor in solution (Figure 2, traces #1A and #2A). The dissociation of IFNAR2-EC from the complex with each interferon was relatively fast and complete, so that no chip surface regeneration was necessary. When injecting IFN-α2c or CM3 during the dissociation phase as soluble competitor to the

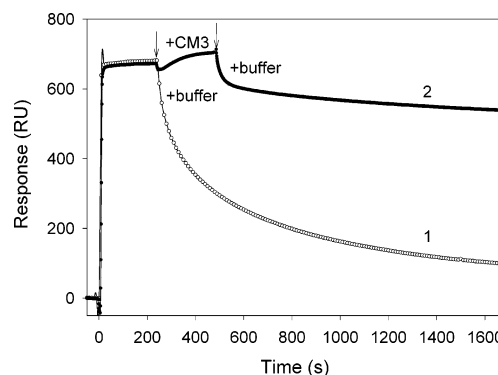FIGURE 3: Effect of CM3 on the interaction of IFN-α2c with the immobilized IFNAR2-EC. 800 nM IFN-α2c was injected onto the chip surfaces to which (1) ~1200 RU IFNAR2-EC or (2) ~1300 RU IFNAR2-EC were immobilized and allowed to dissociate in the absence (1) or presence of 800 nM CM3 (2). Arrows indicate injections of buffer or CM3.

surface immobilized sites, neither competitor accelerated the dissociation rate of the preformed complex of IFNAR2-EC, indicating the absence of rebinding (data not shown). Thus we can conclude that, in the configuration when IFN-α2c or CM3 is immobilized on the chip surface, they interact with IFNAR2-EC similarly and competitively, with association rate constants well below the transport limited regime.

To probe the interaction in more detail, our next step was to change the configuration of the experiments and covalently immobilize IFNAR2-EC on the chip surfaces (to the level of ~1200 RU on surface 1, 1345 RU on surface 2, 1230 RU on surface 3, and 1300 RU on surface 4, respectively), producing active surface site densities similar to those used above. We then examined the receptor interaction with IFN-α2c, CM3, and their equimolar mixture (Figure 2, trace #3, 4, 5, respectively). Again, both interferons were in solution at concentrations sufficient to attain virtual saturation (800 nM). The maximum level of binding (R_{max}) was 690 RU for IFN-α2c (surface 1), 560 RU for CM3 (surface 2), and 530 RU (surface 3) for their equimolar mixture. The value of R_{max} for the mixture did not exceed the R_{max} for any of the interferons alone. These results indicated that interferons did not appear to have independent binding sites on the immobilized IFNAR2-EC, consistent with the solution competition experiment above (Figure 2, traces #1A and #2A).

As can be easily discerned from comparing traces #1 with #3, and #2 with #4 (Figure 2), respectively, the measured binding kinetics changed significantly dependent on whether the IFNAR2-EC was immobilized or chosen as the soluble binding partner. Since a simple bimolecular reaction is invariant when the interacting molecules change place of which is kept in the surface and bulk phase, this indicates that a different, more complicated binding mechanism is present. This is supported by the attempt to quantify this result and fit *ad hoc* the simple pseudo-first-order rate equations to the binding traces: The best-fit apparent rate constants for IFN-α2c/IFNAR2-EC were $K_D^{(app)} = 6.6 \times 10^{-7}$ M and $k_{on}^{(app)} = 4.5 \times 10^4$ M^{-1}s^{-1} when interferon is immobilized, but $K_D^{(app)} = 4.2 \times 10^{-9}$ M and $k_{on}^{(app)} = 9 \times 10^5$ M^{-1}s^{-1} when the receptor is immobilized (fitting several traces at concentrations between 0.8 and 800 nM, data not shown). Similarly, the best-fit off-rate rate constants for CM3/IFNAR2-EC are $k_{off}^{(app)} = 3.0 \times 10^{-2}$ s^{-1} when

interferon is immobilized, but $k_{off}^{(app)} = 7.0 \times 10^{-4}$ s^{-1} when the receptor is immobilized (in the presence of soluble competitor, see below). Further, in each case, there are large residuals of the fit indicating that this model must be rejected. One can conclude that the apparent binding constants from the *ad hoc* fit with the simple bimolecular reaction model do not reflect the true molecular properties, in either case. It is therefore also not surprising that the parameter estimates from the wrong model differ by 2 orders of magnitude from the different experimental designs.

A further observation from the second experiment is that the two interferons interacted with the immobilized receptor differently because the dissociation of IFN-α2c from IFNAR2-EC was significantly faster than that of CM3 and the dissociation of their mixture proceeded at an intermediate rate (Figure 2, traces #3, #4, #5). Interestingly, in this configuration we found a strong rebinding effect in the case of CM3, but only a very weak one in the case of IFN-α2c dissociation from immobilized IFNAR2-EC. The evidence of rebinding was an increase in the rate of interferon dissociation in the presence of the soluble receptor (~30 and ~1.2 times for CM3 and IFN-α2c, respectively, data not shown). Since we have shown the absence of mass transport limitation in the first experiment, the appearance of a strong rebinding effect for CM3 in the configuration of the second experiment, again, cannot be explained on the basis of a simple bimolecular reaction (even allowing for some degree of size- and charge-dependence of the diffusional permeability of the immobilization matrix (*34*)). (One hypothetical effect that may cause such a behavior could be preferential immobilization of IFNAR2-EC in a conformational state (due to secondary or tertiary structural changes) that exhibits a higher on-rate constant for CM3, as compared to the conformational state when the receptor is in free solution.) In addition, as will be described below, there is oligomerization of IFN-α2c in solution, which will be dominant for the surface dissociation behavior due to the high local concentrations in the immobilization matrix of the SPR sensor. Unfortunately, these factors make it impossible to arrive at a reliable and unambiguous quantitative interpretation of the binding kinetics (*35*).

It should be noted that the application of a mixture of the two interferon molecules produced virtually no additional binding to the immobilized IFNAR2-EC that exceeded the binding of one of the interferon molecule alone, indicating competition for sites on the immobilized receptor (Figure 2 trace #5, and Figure 3 trace #2 below). While unexpected on the basis of the ELISA experiments showing only moderate competition, together with the observation that receptor immobilization substantially changed the binding properties in SPR, this result may indicate that differences in the immobilization and/or surface properties may have significant impact on the receptor conformation and consequently binding of soluble IFN. In fact, interpreting the 50% binding level as a gross estimate of an empirical K_D of the ELISA titrations with each individual IFN, the affinity of the receptor in the ELISA experiments is in the high nanomolar and low micromolar range, respectively, which is substantially higher than the SPR results indicate (and as compared estimates of affinity in the literature (*14*)). Therefore, we interpret the receptor state immobilized on the SPR surface more representative of the native state.

In our next experiment, when CM3 was injected over surface 4 that had been saturated with the preformed IFNAR2-EC- IFN-α2c complex (similar to surface 1, 1250 ± 100 RU), the surface-bound complex became significantly stabilized, thus making the binding practically irreversible (Figure 3, trace #2). Some of the dissociation signal can be attributed to the CM3 having formed complexes with empty receptor sites that arose both from incomplete initial saturation and from sites vacated during the initial dissociation of IFN-α2c/receptor complexes. However, if CM3 did not influence the prebound IFN-α2c/receptor complexes as well, then the signals from dissociating CM3/receptor and IFN-α2c/receptor complexes should be strictly additive, and after CM3 application, the kinetic curve of dissociation would be expected to have a slope at least as steep as or steeper than that of trace #1 in Figure 3. The data also cannot be explained by a rebinding-related kinetic exchange mechanism due to the virtual absence of rebinding for IFN-α2c from the immobilized receptor. Therefore, the decrease of the dissociation rate (trace #2) indicated the interaction of CM3 with the preformed IFN-α2c/IFNAR2-EC complex. In order to establish whether this interaction resulted in an exchange of CM3 for IFN-α2c in the IFN/receptor complex, we probed the sensor surface during the slow dissociation by application of the N27 antibody (which also in the SPR experiment binds specifically to IFN-α2c but not to CM3). Under conditions of trace #2 at ~1000 s, N27 gave a large surface binding signal (data not shown), demonstrating that IFN-α2c was still present at the surface after interaction of CM3 with preformed IFN-α2c/IFNAR2-EC. Thus, CM3 does not appear to have completely replaced IFN-α2c on the preformed IFN-α2c/receptor complexes, although contributions via this mechanism cannot be excluded. Possible other mechanisms include induced conformational changes in the IFN-α2c/IFNAR2-EC complex by transient formation of triple complexes in the presence of excess CM3, or, alternatively, a hetero-oligomerization of the IFN/receptor complexes, or more complex schemes involving effects on the self-association of IFN-α2c modulating its binding avidity to the receptor-functionalized SPR surface (see below).

Analysis of IFN-α2c and CM3 Oligomeric State in Solution. In order to gain more insight into the possible binding mechanisms, and the differences in receptor binding observed in SPR, the oligomeric state of both IFN molecules were studied by sedimentation velocity analytical ultracentrifugation.

The rate of migration of the interferons through a centrifugal field was monitored using analytical ultracentrifugation sedimentation velocity (AUC/SV). It is well-established that the rate at which a protein migrates through a centrifugal field is dependent on its mass and shape (*36*). A concentration dependent increase in the sedimentation coefficient would indicate an increase in the protein mass and therefore be diagnostic of self-association. The sedimentation coefficient distribution resulting from the analysis of the CM3 solutions is shown in Figure 4. The major peak had a weight-average sedimentation coefficient (s_w) of 1.9 S and was independent of loading concentration (Figure 4, trace # 1,2), indicating the absence of CM3 self-association.

The sedimentation profile of IFN-α2c was in sharp contrast to CM3. At the lowest IFN-α2c concentration, the $c(s)$ distribution consisted of a single broad peak with a weight-
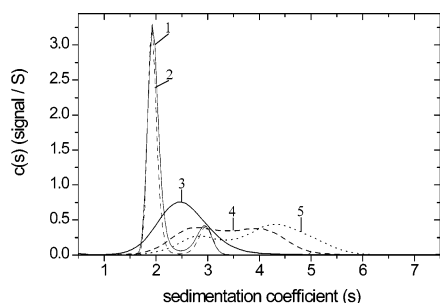
FIGURE 4: Comparison of the sedimentation coefficient distributions for interferons IFN-α2c and CM3. The $c(s)$ distributions for CM3 at loading concentrations of 1.0 mg/mL (trace 1) and 0.5 mg/mL (trace 2) exhibit a major peak at 1.94 S corresponding to CM3 monomer and small fraction of cross-linked dimer at 2.92 S. The $c(s)$ distribution for the IFN-α2c mixtures at 0.1 mg/mL (trace 3), 0.4 mg/mL (trace 4) and 0.8 mg/mL (trace 5) exhibit a concentration-dependent increase in the weight-average sedimentation coefficient indicative of oligomerization.

average sedimentation coefficient (s_w) of 2.6S (Figure 4, trace #3). This value is approximately 35% larger than what was obtained for CM3 monomer. Furthermore, as the loading concentration of IFN-α2c increased, the $c(s)$ distribution became bimodal and the weight average sedimentation coefficient of the entire distribution shifted toward a larger s_w value (3.4 S) indicating an increase of the average molecular weight (Figure 4, trace #4). At the highest concentration, the s_w increased further to 3.9 S, with the fastest moving boundary fraction sedimenting with 4.4 S (Figure 4, trace #5), corresponding to an estimated molar mass ~3.5-fold the monomer mass. The sedimentation velocity data can be described well (rmsd = 0.005) with a global model of Lamm equation solutions (*31*) for rapid monomer−dimer−tetramer self-association with ΔG_{12} = −6.6 kcal/mol corresponding to a K_d value, in three dimensions, of 10 micromolar and ΔG_{24} of = −6.4 kcal/mol (K_d of 15 micromolar in three dimensions).

We studied the presence of heteroassociation of IFN-α2c and CM3 in solution in a simplified assay, by comparing the weight-average s-values of IFN-α2c measured at 0.4 mg/mL with that measured in the presence of additional 0.5 mg/mL CM3. The measured signal-average value of the mixture of 2.86 S is ~5.5% larger than the theoretically expected s_w-value for a non-interacting mixture. This shows that CM3 does not interact or interacts only very weakly with IFN-α2c in solution.

While the free energies of self-association of IFN-α2c are likely too low to influence the initial binding step to the receptor, they support the presence of a more complex binding scheme where self-association of IFN-α2c could contribute to receptor oligomerization processes in the cell membrane. In the present context, the self-association is highly relevant under the conditions of the SPR experiment, for which average concentrations in the high μM range exist in the immobilization matrix on the biosensor surface. This leads to an avidity effect causing the dissociation to proceed at a significantly slower rate constant than the intrinsic chemical dissociation rate constant. As a consequence, an alternative explanation of the effect seen in Figure 3 might be a possible influence of CM3 on the self-association of α2c. Due to the absence of solution interaction between the two IFNs, such an effect either would have to be mediated

by the receptor or would have to involve different conformations of IFN-α2c in complex with the receptor that can interact with CM3.

IFN Receptor Complex in Solution. During ELISA experiments and SPR analysis, proteins were immobilized on the surface. Subsequently, we examined the competition between IFNs for IFNAR2-EC binding in solution. Reaction mixtures, containing different IFN subvariants (Figure 5) after incubation with IFNAR2-EC, were run under native electrophoretic conditions followed by Western blot. If both IFNs (IFN-α2c and CM3) are present at the same time on an IFNAR2-EC complex, it was hypothesized that they would be recognized by both IFN-specific mAbs (1−36: CM3 and N27: IFN-α2c), and that would confirm presence of two different IFNs (IFN-α2c and CM3) on one IFNAR2-EC. Unfortunately, mAb 1/36 showed a diminished activity with CM3 in immunoblot after native electrophoresis (data not shown). Moreover, in electrophoresis under native conditions IFNAR2-EC-CM3 and IFNAR2-EC-IFN-α2c complexes overlapped in the same position of the gel. Thus, it was not possible to distinguish between heterodimeric IFN/receptor complexes composed of IFNAR2-EC and either IFN-α2c or CM3, and trimeric complexes containing the receptor and both interferons using this technique. However as was previously observed (*24*), IFNAR2-EC-IFN-α2c-6-histidine-tag migrates in native electrophoresis at a higher position than IFNAR2-EC-IFN-α2c complex. Therefore, a combination of the above-mentioned IFNs with and without N-terminal 6-histidine tag was used to assess the presence of two different IFNs (IFN-α2c and CM3-6-histidine-tag or IFN-α2c-6-histidine-tag and CM3) on one IFNAR2-EC. As a control, each IFN was subjected to electrophoresis separately. In order to examine if there was a nonspecific interaction between the two IFNs, a mixture of both IFNs were electrophoresed. No interaction was observed under these conditions. Subsequently the IFN/receptor mixture was prepared by incubating each IFN with IFNAR2-EC separately, or by incubating the one IFN with IFNAR2-EC and than adding the second one (preparation described in Experimental Procedures). Two identical sets of samples were examined by electrophoresis. One gel was stained with Sypro Ruby (Figure 5A), and the second one was used for immunoblot (Figures 5B−D). The presence of IFNAR2-EC in IFN receptor complexes was confirmed by anti-IFNAR2-EC mAb 46.10 (Figure 5B); IFN-α2c was detected with mAb N27 (Figure 5C), and the presence of IFNs with 6-histidine-tag was confirmed with HisProbe-HRP recognizing the tag (Figure 5D). The same membrane after stripping was used for all three immunoblots to minimize differences between experiments. After individual incubation of each IFN with IFNAR2-EC the presence of two types of IFN-IFNAR2-EC bands were observed (the first type contained hybrid CM3-6-histidine-tag or IFN-α2c-6-histidine-tag and moves in the gel at a higher position, and the second type contained hybrid CM3 or IFN-α2c and moves in a lower position, Figure 5A, B, C and D). The incubation of two IFNs (with and one without N-terminal 6-histidine-tag) with IFNAR2-EC resulted in formation of two types of IFN-receptor bands {IFNAR2-EC-IFN-(α2c or CM3)-6-histidine-tag complex and IFNAR2-EC-IFN-(α2c or CM3)} complex, Figure 5A, lanes 7, 8, 9, 10). Thus, IFN-α species appear to compete for the receptor binding site. Moreover, IFN-α2c is a better
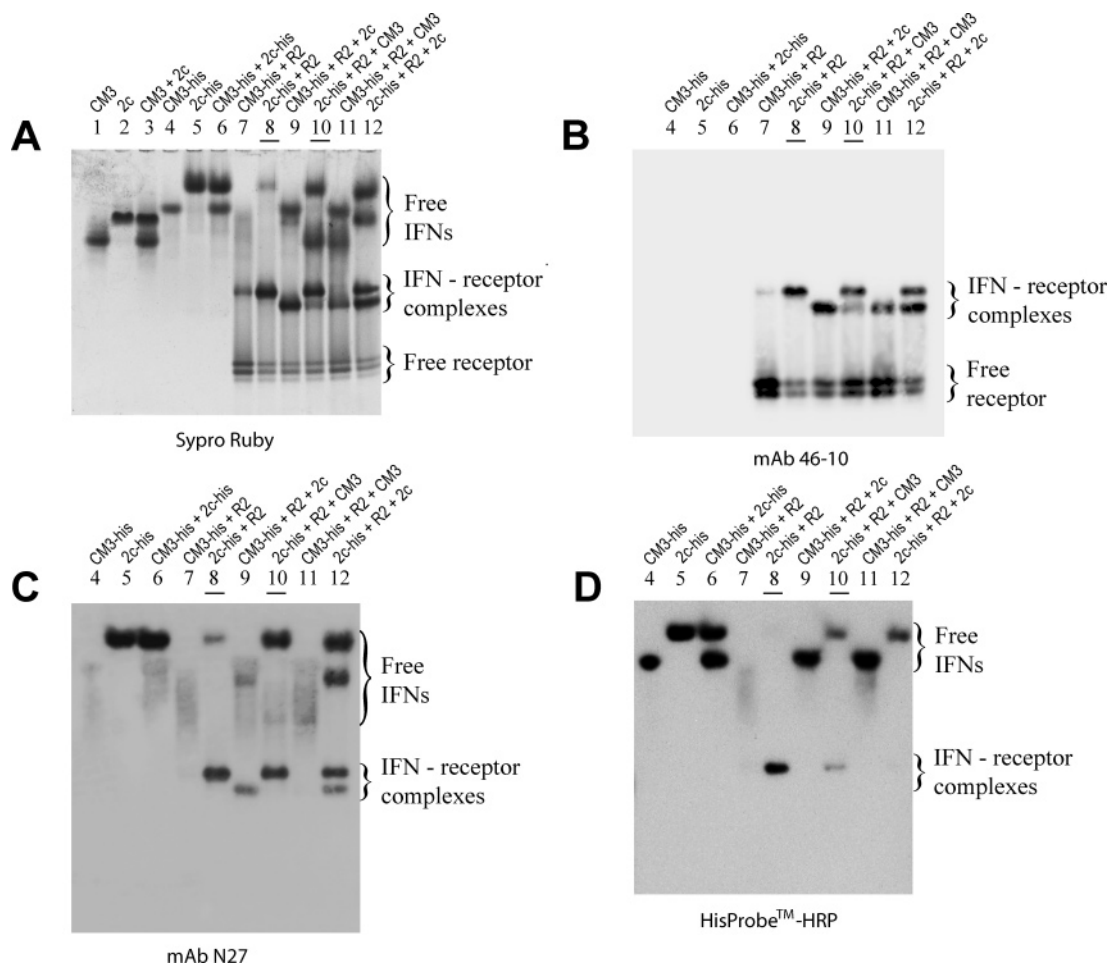
FIGURE 5: Competitive bindings of IFN-α2c and CM3 with IFNAR2-EC in (A) native electrophoresis (10% Tris Glycine gel, stained with Sypro Ruby) and reactivity of mAbs: (B) 46.10, (C) N27, (D) HisProbe-HRP in immunoblot after native electrophoresis. IFNs (0.05 nmol) were incubated with IFNAR2-EC (0.04 nmol) at 37 °C for 1 h, at molar ratio 1.25:1:1.25 (lane 1, CM3; lane 2, IFN-α2c; lane 3, CM3 + IFN-α2c; lane 4, CM-6-histidine-tag; lane 5, IFN-α2c-6-histidine-tag; lane 6, CM3-6-histidine-tag + IFN-α2c-6-histidine-tag; lane 7, CM3-6-histidine-tag + IFNAR2-EC; lane 8, IFN-α2c-6-histidine-tag + IFNAR2-EC; lane 9, CM3-6-histidine-tag + IFNAR2-EC + IFN-α2c; lane 10, IFN-α2c-6-histidine-tag + IFNAR2-EC + CM3; lane 11, CM3-6-histidine-tag + IFNAR2-EC + CM3; lane 12, IFN-α2c-6-histidine-tag + IFNAR2-EC + IFN-α2c.

competitor than CM3, and the N-terminal 6-histidine tag seems not to affect the ability of IFN-α2c to compete for IFNAR2-EC. The results from native electrophoresis showed quantitatively lower amounts of CM3−receptor complex than IFN-α2c−receptor complex (Figure 5A, B), and not even an increase in incubation time or the amount of CM3 would lead to an increase in the quantity of CM3−receptor complexes (Supplement 3, Supporting Information). The presence of a N-terminal 6-histidine tag decreased the competitive ability of CM3 (Figure 5A, lane 11). The most interesting result was observed in immunoblot (Figure 5D, lane 10). Lane 10 should contain IFN−receptor complex formed mostly by IFN-α2c-6-histidine-tag and IFNAR2-EC. However, the HisProbe-HRP had difficulties recognizing this IFN. This band should have been as intense as the band in lane 8 (Figure 5D) (just as the corresponding signals from the N27 antibody recognizing α2c directly are equally intense). This observation raised the possibility that the lesser intensity of band could be due to the presence of the second IFN (CM3). Since we were not able to detect CM3 with specific mAbs in Western blot, we repeated the native electrophoresis described above, cut bands A, B, C from the gel (Figure 6A), performed electroelution, and analyzed the

samples by both electrospray ionization mass spectrometry (ESI-MS, Supplement 4, Supporting Information), and separation of proteins using SDS−PAGE under reducing conditions in 10−20% Tris-glycine gels (Figure 6B). Both analyses confirmed presence of two IFNs (IFN-α2c-6-histidine-tag, CM3) and IFNAR2-EC in the band A (Figures 6A, B, and Supplement 4).

In summary, the native electrophoresis experiments show the IFNs to be largely competitive, but also allowed to detect a population of triple complexes with both IFNs. Considering the much higher protein concentrations used in the electrophoresis assay as compared to the SPR experiments (where CM3 did not lead to additional signal over preformed IFN-α2c/receptor complexes at 800 nM CM3) this would be consistent with a K_D of CM3 for preformed IFN-α2c/receptor complexes in the 10 μM range or higher.
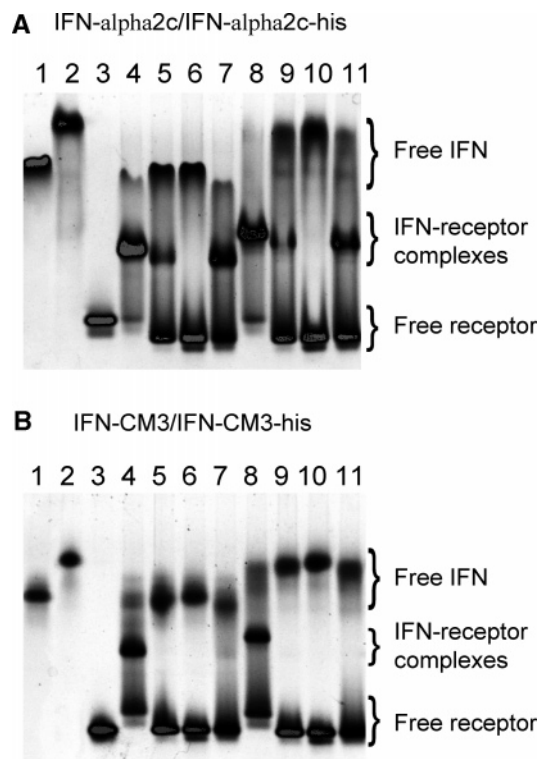
IFNAR2-EC Mutants. IFNAR2-EC mutants used in this part of the study were selected based on sandwich IFN ELISA assays (Drs. G. Schreiber and T. Peleg-Schulman, personal communication). Differences in K_D values between IFN-α2c and CM3 were observed for IFNAR2-EC mutants I105A and M48V (data not shown). The importance of those amino acids for interaction with helices A (45−50) and E
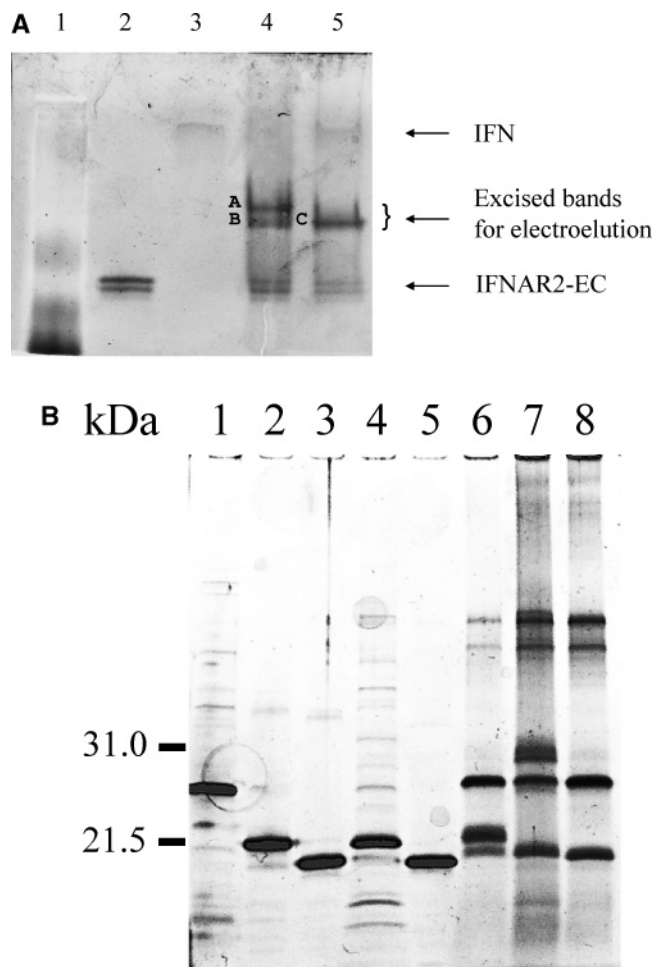
FIGURE 6: A. Native electrophoresis (10% Tris Glycine gel, stained with Sypro Ruby) illustrated bands (A, B, C) were excised for electroelution. IFNs were incubated with IFNAR2-EC at 37 °C for 1 h at molar ratio 1.25:1:1.25 of IFN:IFNAR2-EC:IFN. Lane 1, MW standard; lane 2, IFNAR2-EC; lane 3, IFN-α2c; lane 4, bands A, B IFN-α2c-6-histidine-tag + IFNAR2-EC + CM3; lane 5, bands C CM3-6-histidine-tag + IFNAR2-EC + IFN-α2c. B. Analysis of electroeluted samples in 10−20% SDS Tris Glycine gel (stained with Sypro Ruby) under reducing conditions. Lane 1, IFNAR2-EC (1 μg); lane 2, CM3-6-histidine-tag (1 μg); lane 3, CM3 (1 μg); lane 4, IFN-α2c-6-histidine-tag (1 μg); lane 5, IFN-α2c (1 μg); lane 6, IFN-α2c-6-histidine-tag + IFNAR2-EC + CM3 (band A from native gel, Figure 6A); lane 7, IFN-α2c-6-histidine-tag + IFNAR2-EC + CM3 (band B from native gel, Figure 6A); lane 8, CM3-6-hisitidine-tag + IFNAR2-EC + IFN-α2c (band C from native gel, Figure 6A).

(102−106), as well as loop AB (78−82) of IFN-α2 has also previously been shown by Piehler et al. (1999, 2000). We used native electrophoresis to study differences in binding between CM3 with and without 6-histidine-tag and IFN-α2c with or without 6-histidine-tag and the IFNAR2-EC mutants I47A, I105A and M48V. We observed differences in binding between the aforementioned IFN species for IFNAR2-EC mutants I105A and I47A. IFN-α2c was able to bind to mutants I105A and I47A but CM3 did not form a complex with these receptor mutants (Figure 7A, B). Interestingly enough, these differences had not been observed in the same experiments with IFN-α21b (data not show). Since it was confirmed that helix C is not involved in interaction with IFNAR2-EC (*19*, *23*), these results suggested that mutation in helix C (CM3) could affect IFN-IFNAR2-EC indirectly. The presence or absence of N-terminal 6-histidine tag had

FIGURE 7: A. Binding of IFN-α2c and IFN-α2c-6-histidine-tag with IFNAR2-EC mutants in native electrophoresis (10% Tris Glycine gel, stained with Sypro Ruby). IFNs were incubated with IFNAR2-EC at 37 °C for 1 h at molar ratio 1.25:1. Lane 1, IFN-α2c; lane 2, IFN-α2c-6-histidine-tag; lane 3, IFNAR2-EC; lane 4, IFN-α2c + IFNAR2-EC; lane 5, IFN-α2c + IFNAR2-EC I47A; lane 6, IFN-α2c + IFNAR2-EC M48V; lane 7, IFN-α2c + IFNAR2-EC I105A; lane 8, IFN-α2c-6-histidine-tag + IFNAR2-EC; lane 9, IFN-α2c-6-histidine-tag + IFNAR2-EC I47A; lane 10, IFN-α2c-6-histidine-tag + IFNAR2-EC M48V; lane 11, IFN-α2c-6-histidine-tag + IFNAR2-EC I105A. B. Bindings of CM3 and CM3-6-histidine-tag with IFNAR2-EC mutants in native electrophoresis (10% Tris Glycine gel, stained with Sypro Ruby). IFNs were incubated with IFNAR2-EC at 37 °C for 1 h at molar ratio 1.25:1. Lane 1, CM3; lane 2, CM3-6-histidine-tag; lane 3, IFNAR2-EC; lane 4, CM3 + IFNAR2-EC; lane 5, CM3 + IFNAR2-EC I47A; lane 6, CM3 + IFNAR2-EC M48V; lane 7, CM3 + IFNAR2-EC I105A; lane 8, CM3-6-histidine-tag + IFNAR2-EC; lane 9, CM3-6-histidine-tag + IFNAR2-EC I47A; lane 10, CM3-6-histidine-tag + IFNAR2-EC M48V; lane 11, CM3-6-histidine-tag + IFNAR2-EC I105A.

no effect on behavior of CM3. The above-described results show that different IFNs could utilize different amino acids on IFNAR2-EC for binding.

Neutralization of Antiproliferative Activities of Interferons on Daudi Cells with Soluble IFNAR2-EC. Results of the neutralization assay show that IFNAR2-EC neutralized both IFNs to the same degree, suggesting that IFN-α2c and CM3 are binding to IFNAR2-EC with similar affinity. This observation led to the conclusion that differences between IFN-α2c and CM3 in antiproliferative assay are not due to problems in interaction with IFNAR2. Moreover, incubation of a mixture of IFNs with IFNAR2-EC in cell-based experiments supports evidence that CM3 competes less effectively for IFNAR2-EC than IFN-α2c, by virtue of the fact that neutralizing effect of IFNAR2-EC on IFN-α2c was not decreased by the presence of CM3 (Table 1). Thus, lower competition of CM3 could be explained by utilization of different amino acids in the binding region of IFNAR2-EC rather than differences in affinity.

Table 1: Neutralization of Antiproliferative (AP) Activities of Interferons with IFNAR2-EC on Daudi Cells at 48 h Time Point[a]

IFNs	AP (ng/mL)	AP (ng/mL) with IFNAR2-EC
IFN-α2c	0.03	0.1
CM3	0.4	1.4
IFN-α2c + CM3	0.04	0.4

[a] Concentration that inhibits cell growth by 50%. Daudi cells were mock-treated or treated with IFN-α2c, CM3, or their mixture (tenfold dilutions from initial concentrations of 360 ng/mL for single IFN, or equimolar IFN mixture) with or without IFNAR2-EC (at a constant concentration of 5 μg/mL). Data shown are from one representative experiment.

DISCUSSION

The IFN/receptor interaction is critical in determining the extent of the subsequent biological response (*5*, *37*, *38*). Differences in spectra of biological activities among members of the IFN-α family indicate that each subtype could exhibit differences in receptor binding and/or intracellular signaling.

Our previous results showed that hybrid IFNs with N-terminal portion derived from IFN-α21b competed poorly with IFN-α2b for cellular binding (*12*, *17*). CM3 is one of these hybrids, and also has a mutation in helix C (Y86K). Structural changes in helix C may influence interaction with IFNAR1, a component of the type I interferon receptor which is considered important for IFN antiproliferative activity (*19*). This could explain the tenfold lower antiproliferative activity of CM3 than that of IFN-α2c in 48 h antiproliferative assay. It did however not explain the 800-fold lower ability of CM3 (with 6-histidine tag) to compete with IFN-α2c (with 6-histidine tag) for receptor binding site (*17*).

This observation raised the question, whether interaction among two individual IFN-αs and IFNAR2-EC contributes to the observed poor competition. To explore this question, we analyzed the binding of IFN-α2c and hybrid CM3 with IFNAR2-EC using defined anti-IFN mAbs in competitive binding ELISA, native electrophoresis followed by Western blot, ESI-MS, SPR analysis and neutralization assay.

The data from competitive binding ELISA appear to show that two IFN-α subtypes could bind simultaneously to IFNAR2-EC without significantly affecting each other's binding to IFNAR2-EC. Only IFNs with N-terminal 6-histidine-tag were used in all ELISA experiment, due to the fact that mAbs only recognized IFNs with 6-histidine-tag after binding to IFNAR2-EC. This could be explained by an influence of the 6-histidine-tag on the IFN structure (*24*).

In order to approach the surface binding observed by ELISA in a more quantitative way, further analysis of the interaction of IFN-α2c and CM3 with IFNAR2-EC was done using SPR optical biosensing. To exclude any negative effect a tag might have on interaction, we used IFNs without N-terminal 6-histidine-tag in these experiments. SPR optical biosensing is a technology that provides real time information on the course of the interaction, and is similar to ELISA in that it requires the immobilization of one of the interacting compounds. It does not, however, require the use of antibodies. Because of the surface, two experimental designs were possible: one, where the interferons were covalently attached to the chip surface, while the receptor was in solution, and the other, with the reverse configuration. Strikingly different binding curves were detected in the different configurations, pointing to a more complex interaction mechanism.

In the configurations where IFN-α2c or CM3 were immobilized on the chip surface, their interaction with IFNAR2-EC that was in solution was similar. Neither of the soluble interferons had any influence on the kinetics of dissociation of the prebound receptor. In the configuration in which IFNAR2-EC was immobilized, IFN-α2c and CM3 each interacted differently with the receptor and CM3 affected the kinetics of dissociation of the preformed IFN-α2c/receptor complex. One could hypothesize that during the formation of the interferon-surface-bound receptor complexes, different interferons might undergo small conformational changes, which may be mutually influenced by a transient interaction. With immobilized interferons, the immobilization constraints might prohibit the necessary conformational flexibility. Alternatively, lateral association or oligomerization of the receptor−interferon complex produced by their close proximity on the sensor chip surface might also play a role. This is emphasized by our observation from sedimentation velocity of the self-association in solution of IFN-α2c, but no detectable self-association of CM3. While the SPR data did not confirm the presence of two individual IFN-αs on IFNAR2-EC, they showed that both IFNs influence each other during this interaction. The differences in results between ELISA and SPR could be due to the fact that these methods use different surfaces for immobilization of proteins. This could potentially lead to different results regarding the conformation and aggregation state of the surface-bound molecules. Further, the molecules used were slightly different (his-tag in ELISA versus no his-tag in SPR).

ELISA experiments and SPR analysis required immobilizing the proteins onto a surface. Thus the surface could contribute to structural changes of the proteins. To eliminate that possibility, protein−protein interactions were studied in solution, and detected by native electrophoresis and immunoblot. These experiments showed competition between IFN-α2c and CM3 (with or without 6-histidine tag) for IFNAR2-EC. Moreover, ESI-MS analysis of bands representing IFN−receptor complexes that were cut from native PAGE gels confirmed the presence of two IFNs with the IFNAR2-EC at the same time in the band A. These results suggested that two IFNs could bind directly to IFNAR2-EC. However, binding of CM3 to the IFNAR2-EC portion of the IFNAR2-EC/IFN-α2c complex is probably weak and transient, since it is not able to release IFN-α2c from IFNAR2-EC interaction effectively. The presence of CM3 could affect the conformation of IFN-α2c, which could be an additional explanation why HisProbe-HRP recognized IFN-α2c in the complex less effectively. Further studies and the use of different experimental approaches will be necessary to gain a detailed understanding of these interactions.

The generally observed lower quantity of CM3 (with or without 6-histidine-tag) receptor complexes could be explained by conditions in native electrophoresis that may cause some structural changes on CM3 molecule, which then could reduce interaction with IFNAR2-EC.

Experiments using IFNAR2-EC mutants in native electrophoresis showed that IFNAR2-EC mutations in positions 105 (I105A) and 47 (I47A) completely prevented interaction between CM3 (with or without 6-histidine tag) and the receptor subunit. These results provide evidence that CM3

(with or without 6-histidine tag) and IFN-α2c (with or without 6-histidine tag) could use different amino acids within the binding domain of IFNAR2-EC. Similar results had been observed for IFN-α2c versus IFN-β, where mutating IFNAR2-EC (W102A) proved to be most destructive for IFN-β binding (*22*, *39*). Because IFNs mutually influence each other during competition, binding domains are probably in close proximity or overlapping (*22*).

Cell-based neutralization assays with IFNAR2-EC show the same neutralization effect on CM3 and IFN-α2c. Thus the utilization of different amino acids in the binding region of IFNAR2 could help explain the better competitive ability of IFN-α2c compared to that of CM3. Moreover, these results strengthen evidence that the mutation in helix C had no impact on interaction with IFNAR2. The difference between the two IFNs observed in antiproliferative assay could be a consequence of interaction with IFNAR1 (*19*).

In conclusion, the results of this study show the complexity of the interaction among different IFN-α subtypes during the process of binding to IFNAR2-EC. They underscore the importance of the differences in interaction on the amino acid level during this process, which could help understand the significance of the existence of the various IFN-αs subtypes.

SUPPORTING INFORMATION AVAILABLE

Supplement 1, comparison of the reactivity of IFN-α2c-6-histidine-tag and CM3-6-histidine-tag with monoclonal antibodies in solid phase IFN ELISA and in sandwich IFNAR2-EC ELISA I; Supplement 2, time-dependent binding of IFN-α2c-6-histidine-tag and CM3-6-histidine-tag to IFNAR2-EC in sandwich IFNAR2-EC ELISA II; Supplement 3, saturation of IFNAR2-EC with CM3 in native electrophoresis; Supplement 4, analysis of samples by electrospray ionization mass spectrometry (ESI-MS). This material is available free of charge via the Internet at http://pubs.acs.org.

REFERENCES

1. La Fleur, D. W., Nardelli, B., Tsareva, T., Mather, D., Feng, P., Semenuk, M., Taylor, K., Buergin, M., Chinchilla, D., Roshke, V., Chen, G., Ruben, S. M., Pita, P. M., Coleman, T. A., and Moore, P. A. (2001) Interferon−kappa, a novel type I interferon expressed in human keratinocytes, *J. Biol. Chem. 276*, 39765−39771.
2. Conclin, D. C., Grant, F. J., Rixon, M. W., and Kindsvogel, W. (2002) Interferon-ε, U.S. Patent 6329175.
3. Kontsek, P., Karayianni-Vasconcelos, G., and Kontsekova, E. (2003) The human interferon system: characterization and classification after discovery of novel members, *Acta Virol. 47*, 201−215.
4. Sen, G. C. (2001) Viruses and interferons, *Annu. Rev. Microbiol. 55*, 255−281.
5. Kontsek, P. (1994) Human type I interferons: structure and function, *Acta Virol. 38*, 345−360.
6. Diaz, M. O., Bohlander, S., and Allen, G. (1996) Nomenclature of the human interferon genes, *J. Interferon Cytokine Res. 16*, 179−180.
7. Bekisz, J., Schmeisser, H., Hernandez, J., Goldman, N. D., and Zoon, K. C. (2004) Human IFNs α, β, ω. Review, *Growth Factor 4*, 243−251.
8. Pestka, S. (1983) The human interferons from protein purification and sequence to cloning and expression: before, between and beyond, *Arch. Biochem. Biophys. 221*, 585−589.
9. Zoon, K. C., Miller, D., Bekisz, J., zur Nedden, D., Enterline, J. C., Nguyen, N. Y., and Hu, R. (1992) Purification and characterization of multiple components of human lymphoblastoid interferon-α, *J. Biol. Chem. 267*, 15210−15216.
10. Takaoka, A., and Yanai, H. (2006) Interferon signaling network in innate defence, *Cell. Microbiol. 8*, 907−922.
11. Nyman, T. A., Tolo, H., Parkkinen, J., and Kalkkinen, N. (1998) Identification of nine interferon-alpha subtypes produced by Sendai virus-induced human peripheral blood leucocytes, *Biochem. J. 329*, 295−302.
12. Hu, R., Gan, Y., Liu, J., Miller, D., and Zoon, K. C. (1993) Evidence for multiple binding sites for several components of human lymphoblastoid interferon-α, *J. Biol. Chem. 268*, 12591−12595.
13. Novick, D., Cohen, B., and Rubinstein, M. (1994) The human interferon α/β receptor: Characterization and molecular cloning, *Cell 77*, 391−400.
14. Jaks, E., Gavutis, M., Uze, G., Martal, J., and Piehler, J. (2006) Differential receptor subunit affinities of type I interferons govern differential signal activation, *J. Mol. Biol. 2*, 525−539.
15. Mogensen, K. E., Lewerenz, M., Reboul, J., Lutfalla, G., and Uze, G. (1999) The type I interferon receptor: Structure, function, and evolution of a family business, *J. Interferon Cytokine Res. 19*, 1069−1098.
16. Uze, G., Lutfalla, G., and Gresser, I. (1990) Genetic transfer of a functional human interferon a receptor into mouse cells: Cloning and expression of its c DNA, *Cell 60*, 225−234.
17. Hu, R., Bekisz, J., Schmeisser, H., McPhie, P., and Zoon, K. (2001) Human IFN-α protein engineering: The amino acid residues at positions 86 and 90 are important for antiproliferative activity, *J. Immunol. 167*, 1482−1489.
18. Jaitin, D. A., Roisman, L. C., Jaks, E., Gavutis, M., Piehler, J., Van der Heyden, J., Uze, G., and Schreiber, G. (2006) Inquiring into the differential action of interferons (IFNs): an IFN-alpha2 mutant with enhanced affinity to IFNAR1 is functionally similar to IFN-beta, *Mol. Cell Biol. 5*, 1888−1897.
19. Roisman, L. C., Jaitin, D. A., Baker, D. P., and Schreiber, G. (2005) Mutational analysis of the IFNAR1 binding site on IFNα2 reveals the architecture of a weak ligand-receptor binding site, *J. Mol. Biol. 353*, 271−281.
20. Cajean-Feroldi, C., Nosal, F., Nardeus, P. C., Gallet, X., Guymarho, J., Baychelier, F., Sempe, P., Tovey, M. G., Escary, J. L., and Eid, P. (2004) Identification of residues of the IFNAR1 chain of the type I human interferon receptor critical for ligand binding and biological activity, *Biochmemistry 39*, 12498−12512.
21. Piehler, J., and Schreiber, G. (1999) Biophysical analysis of the interaction of human Ifnar2 expressed in E. coli with IFN-α2, *J. Mol. Biol. 289*, 57−67.
22. Piehler, J., and Schreiber, G. (1999) Mutational and structural analysis of the binding interface between type I IFNs and their receptor IFNAR2, *J. Mol. Biol. 294*, 223−237.
23. Piehler, J., Roisman, L. C., and Schreiber, G. (2000) New structural and functional aspects of the type I interferon-receptor interaction revealed by comprehensive mutational analysis of the binding interface, *J. Biol. Chem. 275*, 40425−40433.
24. Schmeisser, H., Kontsek, P., Esposito, D., Gillette, W., Schreiber, G., and Zoon, K. C. (2006) Binding characteristids of interferon-a

subvariants to IFNAR2-EC and influence of the 6-histidine tag. Accepted in, *J. Interferon Cytokine Res. 26*, 866−876.

25. Ellman, G. L. (1959) Tissue sulfhydryl groups, *Arch. Biochem. Biophys. 82*, 70−77.

26. Kontsek, P., Borecky, L., Zav'yalov, V. P., and Maiorov, V. A. (1993) Peptide-mapping of three neutralizing epitopes into predicted biologically active sites of human interferon-α2, *Immunol. Lett. 35*, 281−284.

27. Alexenko, A. P., Izotova, L. S., Kostrov, S. V., and Strongin, A. Y. (1991) Mapping of an epitope of human leukocyte interferon A which is recognized by the murine monoclonal antibody NK2, *Biomed. Sci. 2*, 403−409.

28. Kontsek, P., Borecky, L., Kontsekova, E., Kolcunova, A., Novak, M., Zav'yalov, V. P., and Maiorov, V. A. (1992) Immunodominant structures in the aminoterminal portion of human interferon-α1, *Mol. Immunol. 29*, 863−870.

29. Arnheiter, H., Thomas, R. M., Leist, T., Fountoulakis, M., and Gutter, B. (1981) Physiochemical and antigenic properties of synthetic fragments of human leukocyte interferon, *Nature 294*, 278−280.

30. Svitel, J., Balbo, A., Mariuzza, R. A., Gonzales, N. R., and Schuck, P. (2003) Combined affinity and rate constant distributions of ligand populations from experimental surface binding kinetics and equilibria, *Biophys. J. 84*, 4062−4077.

31. Dam, J., Velikovsky, C. A., Mariuzza, R. A., Urbanke, C., and Schuck, P. (2005) Sedimentation velocity analysis of heterogeneous protein-protein interaction: Lamm equation modeling and sedimentation coefficient distributions c(s), *Biophys. J. 89*, 619−634.

32. Yeh, T. J., Mc Bridge, P. T., Overall, J. C., Jr., and Green, J. A. (1982) Automated, quantitative cytopathic effect reduction assay for interferon, *J. Clin. Microbiol. 16*, 413−415.

33. McKenna, S. D., Vergilis, K., Arulanandam, A. R. N., Weiser, W. Y., Nabioullin, R., and Tepper, M. A. (2004) Formation of human IFN-β complex with the soluble type I interferon receptor IFNAR2 leads to enhanced IFN stability, pharmacokinetics, and antitumor activity in xenografted SCID mice, *J. Interferon Cytokine Res. 24*, 119−129.

34. Schuck, P. (1996) Kinetics of ligand binding to receptor immobilized in a polymer matrix, as detected with an evanescent wave biosensor. I. A computer simulation of the influence of mass transport, *Biophys. J. 70*, 1230−1249.

35. Schuck, P. (1997) Use of surface plasmon resonance to probe the equilibrium and dynamic aspects of interactions between biological macromolecules, *Annu. Rev. Biophys. Biomol. Struct. 26*, 541−555.

36. Lebowitz, J., Lewis, M. S., and Schuck, P. (2002) Modern analytical ultracentrifugation in protein science: A tutorial review, *Protein Sci. 11*, 2067−2079.

37. Deonarain, R., Chan, D. C. M., Platanias, L. C., and Fish, E. N. (2002) Interferon-alpha/beta receptor interactions: A complex story unfolding, *Curr. Pharm. Des. 8*, 2131−2137.

38. Hu, R., Bekisz, J., Hayes, M., Audet, S., Beeler, J., Petricoin, E., and Zoon, K. C. (1999) Divergence of binding, signaling, and biological responses to recombinant human hybrid IFN, *J. Immunol. 163*, 854−860.

39. Peleg-Shulman, T., Roisman, L. C., Zupkovitz, G., and Schreiber, G. (2004) Optimizing the binding affinity of a carrier protein: a case study on the interaction between soluble IFNAR2 and interferon beta, *J. Biol. Chem. 17*, 18046−18053.